DOI: 10.3901/CJME.2010.05.***, available online at www.cjmenet.com; www.cjmenet.com.cn

Modeling and Analysis of Novel Integrated Radial Hybrid Magnetic Bearing for Magnetic Bearing Reaction Wheel

HAN Bangcheng[1, 2, *]

1 *Key Laboratory of Novel Inertial Instrument & Navigation System Technology of Fundamental Science for National Defense, Beihang University, Beijing 100191, China*
2 *School of Instrument Science and Opto-electronics Engineering, Beihang University, Beijing 100191, China*

Received February 10, 2009; revised July 8, 2010; accepted July , 2010; published electronically July , 2010

Abstract: Conventional ball bearing reaction wheel used to control the attitude of spacecraft can't absorb the centrifugal force caused by imbalance of the wheel rotor, and there will be a torque spike at zero speed, which seriously influences the accuracy and stability of spacecraft attitude control. Compared with traditional ball-bearing wheel, noncontact and lubrication are the remarkable features of the magnetic bearing reaction wheel, and which can solve the high precision problems of wheel. In general, two radial magnetic bearings are needed in magnetic bearing wheel, and the design results in a relatively large axial dimension and higher momentum-to-mass ratios. In this paper, a new type of magnetic bearing reaction wheel(MBRW) is introduced for satellite attitude control, and a novel integrated radial hybrid magnetic bearing(RHMB) with permanent magnet bias is designed to reduce the mass and minimize the size of the MBRW, etc. The equivalent magnetic circuit model for the RHMB is presented and a solution is found. The stiffness model is also presented, including current stiffness, position negative stiffness, as well as tilting current stiffness, tilting angular position negative stiffness, force and moment equilibrium equations. The design parameters of the RHMB are given according to the requirement of the MBRW with angular momentum of 30 N • m • s when the rotation speed of rotor reaches to 5 kr/min. The nonlinearity of the RHMB is shown by using the characteristic curves of force–control current–position, current stiffness, position stiffness, moment–control current–angular displacement, tilting current stiffness and tilting angular position stiffness considering all the rotor position within the clearance space and the control current. The proposed research ensures the performance of the radial magnetic bearing with permanent magnet bias, and provides theory basis for design of the magnetic bearing wheel.

Key words: magnetic bearing reaction wheel, radial hybrid magnetic bearing, equivalent magnetic circuit, current stiffness, position negative stiffness, tilting current stiffness, tilting angular position stiffness

1 Introduction

The current spacecraft attitude control systems or spacecraft pointing systems rely almost exclusively upon some type of mechanical rolling element bearings. Inherent in these systems is the need for reliable and long-life bearing and lubrication systems, and there will be a torque spike at zero speed for ball-bearing wheel[1–2]. Requirements are calling for increasingly higher reliability and longer lifetime while imposing higher performance requirements. Compared with traditional ball-bearing wheel, to support a wheel magnetically in five degrees of freedom(DOF), no contact and lubrication are the remarkable features of the magnetic bearings, which solve the long-life and high precision problems of wheel[3–4]. Magnetic bearings have very low levels of parasitic drag torque and force, especially at lower speeds, and can utilize microprocessors and feedback to control or restrain vibration in a manner that is unique from all other types of bearings. The advanced magnetic bearing wheel has been flight-proven on the SPOT (Satellite Pour l'Observation de la Terre) satellite[5]. The first to fly in Europe was a French 1-DOF wheel in SPOT 1, SPOT 2 and SPOT 3 and in ERS 1 and ERS 2. And then, the 2-DOF wheels were developed for to suppress the axial dimension of the wheel[6].

Magnetic bearing wheel is supported by radial magnetic bearing and axial magnetic bearing in five DOFs. The radial magnetic bearing will affect the stability, control precision and nonlinearity etc. of the MBRW. The radial translation and tilt about two axes orthogonal to the spin axis are controlled by radial magnetic bearing for lots of magnetic bearing wheels[7]. Two radial magnetic bearings are needed in this type of magnetic bearing wheel[2, 6, 8–9]. The design results in a relatively large axial dimension and higher momentum-to-mass ratios. The tilt about two axes orthogonal to the spin axis is controlled by passive means[10–11]. Also, this configuration makes the passive control of oscillations difficult and low control precision

* Corresponding author. E-mail: hanbangcheng@buaa.edu.cn
This project is supported by National Natural Science Foundation of China (Grant No. 60704025)

comparing to the active means. And most literatures described the control method and the magnetic bearing wheel system. But few literatures on the model and analysis of the radial magnetic bearing with permanent magnetic bias are published, especially on the analysis of the tilting stiffness.

To avoid these problems, a compact magnetic bearing reaction wheel(MBRW) (rating angular momentum is 30 N • m • s when the rotation speed of rotor reaches to 5 kr/min) is described based on a novel integrated radial hybrid magnetic bearing with permanent magnets providing a steady-state bias flux for suspension and the electromagnets providing the necessary stability and control. This combination resulted in not only a lower power consumption bearing, but also a lighter bearing because less iron is needed in the magnetic circuit. The structure of the radial hybrid magnetic bearing(RHMB) is introduced, and its equivalent magnetic circuit model is presented. And the stiffness model is also given through the current stiffness, position negative stiffness, as well as tilting current stiffness, tilting angular position negative stiffness, and the force and moment equilibrium equation. The design parameters of the RHMB are given according to the requirement of a type of MBRW. The nonlinearity of the RHMB is shown by using the characteristic curves of force–current–position, current stiffness, position stiffness, moment–current–angular displacement, tilting current stiffness and tilting angular position stiffness considering all the rotor position within the clearance space and the control current.

This paper includes the following three main levels: (1) Physical descriptions of the MBRW and the RHMB; (2) The magnetic circuit model of the RHMB; (3) The parameters design and performance analysis for the RHMB. In section 2, a novel MBRW with RHMB is described. Consequently, the magnetic circuit model of the RHMB is presented in section 3. The parameters design and performance analysis for the RHMB are presented in section 4, followed by discussions and conclusions.

2 Physical Descriptions of the MBRW and the RHMB

Fig. 1 illustrates the configuration of the magnetically suspended flywheel. The rotational speed of magnetically suspended rotor is from −5 kr/min to 5 kr/min (rating angular momentum is 30 N • m• s), the maximum rotational speed can reach to 10 kr/min, and is supported by radial hybrid magnetic bearing and thrust hybrid magnetic bearing. The 2-DOF, radial translation along the two axes orthogonal to the spin axis, and the 2-DOF, tilt about two axes orthogonal, are controlled by the RHMB. The axial translation is controlled by thrust hybrid magnetic bearing with permanent magnet bias. The 5-DOF wheel can embody all the capabilities of magnetic suspension. The sixth DOF (i.e., spin) is controlled by active means, using a brushless ironless DC motor.

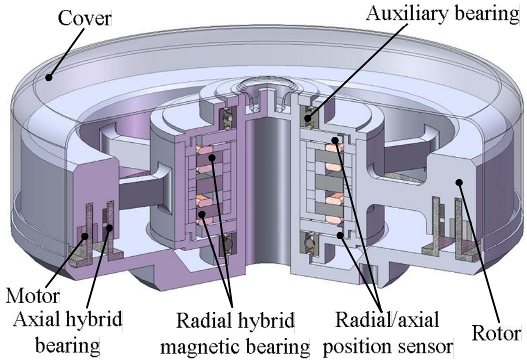

Fig. 1. Configuration of the magnetically suspended flywheel

At wheel level, subassemblies of the MSRW are the following.

(1) The RHMB stabilizes the rotor on the two axes orthogonal to the spin axis and creates a tilting stiffness to restrain the rotor when subjected to gyroscopic torque, with permanent magnets providing a steady-state bias flux for suspension and the electromagnets providing the necessary stability and control, which resulted in not only a lower power consumption bearing, but also a lighter bearing because less iron is needed in the magnetic circuit. The radial hybrid magnetic bearing is also developed to suppress the axial dimension of the wheel.

(2) The thrust hybrid magnetic bearing exerts restoring forces on the rotor at axial translation with permanent magnets providing a steady-state bias flux for suspension and the electromagnets providing the necessary stability and control.

(3) The radial/axial position sensor, using eddy current type position sensor, detects the radial position and axial position of the suspended rotor and provides the necessary error correction signals which are used for the stabilization of the rotor.

(4) The drive motor, for maintenance of the wheel’s rotor’s angular rate, is a brushless ironless DC multiple type in which phase commutation relies on digital Hall-effect sensors, integrated into the rotor rim. The permanent magnets of the motor are attached to the rotor rim and thus make a useful contribution to the rotating mass.

(5) Auxiliary bearings, using ball bearing, provide a safe landing of the rotor in the event of a failure occurring in the suspension electronic, or loss of power supply while rotating. They provide for radial support and axial support.

The construct of the RHMB, which consists of rotor and stator, is shown in Fig. 2 and Fig. 3. The rotor consists of three soft magnetic axisymmetric pieces and an axisymmetric return ring (made of soft magnetic material). The stator consists of three soft magnetic pieces (they each have four equally spaced electromagnet poles and four coils on upper and lower pieces, which are distributed at intervals of 90° around the stator iron), two axially polarized permanent-magnet rings, and three axisymmetric return rings (also made of soft magnetic material). The feature leads to a very compact design to suppress the axial dimension of the MBRW. The two opposing magnetic poles allow control forces on the axes perpendicular to the spin axis respectively taking accounting of linearization effect. This is beneficial for the position control. The permanent magnet(PM) sends radial directed "bias" flux across the angular air gaps in opposite directions toward the rotor iron. The control flux originates from the control coils. It allows adding or subtracting flux into the air gaps according to the sign of the current, and then the restoring force and/or moment will be produced to stabilize the rotor on the two axes orthogonal to the spin axis and/or creates a tilting stiffness to restrain the rotor when it is subjected to gyroscopic torque according to the rotor position. The control flux and the bias flux pass through the different magnetic circuit, which resulted in lower power consumption and higher performance.

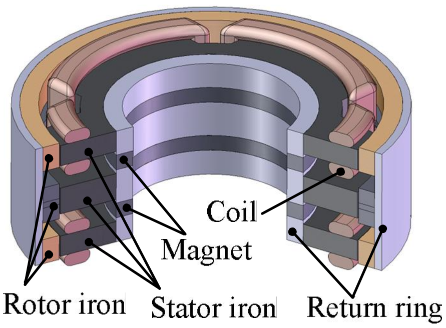

Fig. 2. Configuration of the RHMB

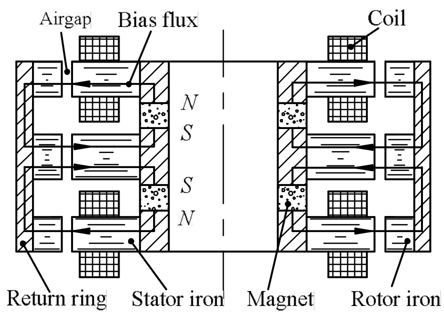

(a) Bias flux

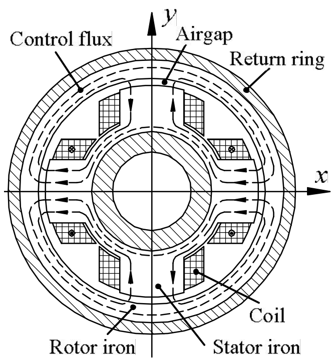

(b) Control flux

Fig. 3. Structure and magnetic circuit of RHMB

3 Magnetic Circuit Model of the RHMB

3.1 Magnetic circuit model of the RHMB

According to the structure of the RHMB and its magnetic circuit (Fig. 3), the magnetic resistance of the iron path and flux leakage is neglected (the permeability of the iron is assumed to be infinite), and the equivalent magnetic circuit of the RHMB can be gained and is shown in Fig. 4. The control flux and the bias flux pass through the different magnetic circuit. Fig. 5 shows the equivalent permanent bias circuit for two permanent-magnet rings. Fig. 6 shows the equivalent control circuit for upper soft magnetic piece and lower soft magnetic piece.

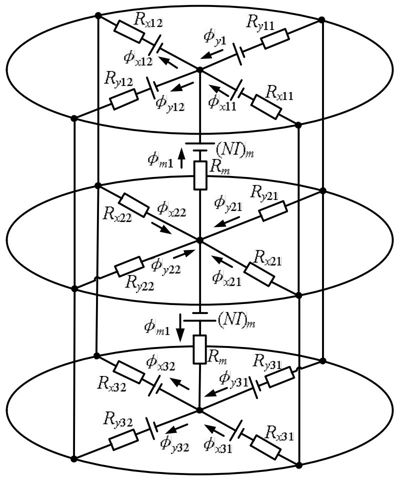

Fig. 4. Equivalent magnetic circuit of RHMB

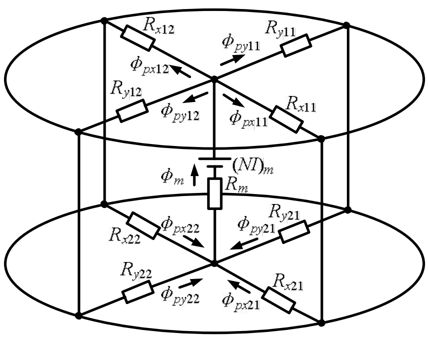

(a) For upper permanent-magnet ring

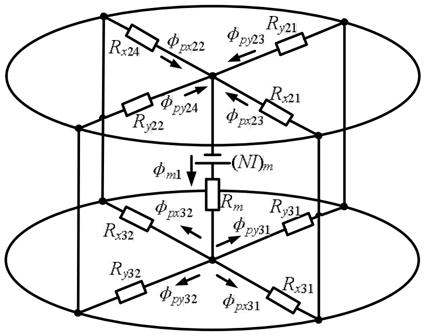

(b) For lower permanent-magnet ring

Fig. 5. Equivalent permanent bias circuits for upper and lower permanent-magnet rings

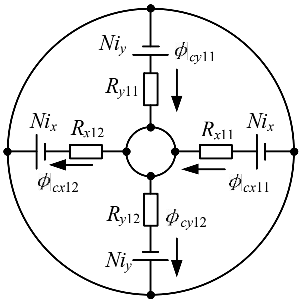

(a) For upper soft magnetic pieces

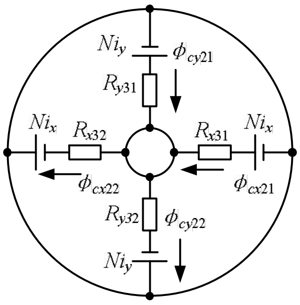

(b) For lower soft magnetic pieces

Fig. 6. Equivalent control circuits for upper and lower soft magnetic pieces

3.2 Model of the RHMB for radial translation

The RHMB control the movement of the rotor along x and y axes orthogonal to the spin axis. When the rotor deviates radially from its "suspended" position at x axis direction (the magnetomotive force at y-axis, Ni_y=0), the net force at the x-axis, F_x, can be written as Eq. (1) according to the structure of RHMB (Fig. 3) and its equivalent magnetic circuits (Fig. 4–Fig. 6):

$$F_x = \frac{\phi_{x11}^2}{\mu_0 A} - \frac{\phi_{x12}^2}{\mu_0 A} + \frac{\phi_{x21}^2}{\mu_0 A} - \frac{\phi_{x22}^2}{\mu_0 A} + \frac{\phi_{x31}^2}{\mu_0 A} - \frac{\phi_{x32}^2}{\mu_0 A}, \tag{1}$$

where the constant μ_0 is the permeability of free space and is equal to 0.4π μH/m; A is the area of the magnetic pole face; ϕ_{x11}, ϕ_{x12}, ϕ_{x21}, ϕ_{x22}, ϕ_{x31} and ϕ_{x32} are the flux passing radial through the air gaps on x-axis, and they can be written as follows:

$$\begin{cases} \phi_{x11} = \phi_{px11} + \phi_{cx11}, \\ \phi_{x12} = \phi_{px12} - \phi_{cx12}, \\ \phi_{x21} = \phi_{px21} + \phi_{px23}, \\ \phi_{x22} = \phi_{px22} + \phi_{px24}, \\ \phi_{x31} = \phi_{px31} + \phi_{cx21}, \\ \phi_{x32} = \phi_{px32} - \phi_{cx22}, \end{cases} \tag{2}$$

where ϕ_{px11}, ϕ_{px12}, ϕ_{px21}, ϕ_{px22}, ϕ_{px23}, ϕ_{px24}, ϕ_{px31} and ϕ_{px32} are the bias flux passing radially through the air gaps on x-axis, which produced by two permanent-magnet rings. ϕ_{cx1}, ϕ_{cx2}, ϕ_{cx21} and ϕ_{cx22} are the control flux of magnetic circuits passing radial through the air gaps on x-axis. The relation of the bias flux is $\phi_{px11}=\phi_{px31}$, $\phi_{px12}=\phi_{px32}$, $\phi_{px21}=\phi_{px23}$, $\phi_{px22}=\phi_{px24}$ when the rotor translates at x-axis. The relationship of the control flux is $\phi_{cx11}=\phi_{cx21}$ and $\phi_{cx12}=\phi_{cx22}$ when the rotor translates at x-axis. So Eq. (1) can be simplified by

$$F_x = 2\left(\frac{\phi_{x11}^2}{\mu_0 A} - \frac{\phi_{x12}^2}{\mu_0 A} + \frac{\phi_{px21}^2}{\mu_0 A} - \frac{\phi_{px22}^2}{\mu_0 A}\right). \tag{3}$$

The bias flux in Fig. 5 can be calculated respectively by Eq. (4):

$$\begin{cases} \phi_{px11} = \dfrac{(NI)_\mathrm{m}}{R_\mathrm{m} + R_1 + R_2} \dfrac{R_1}{R_{x11}}, \\ \phi_{px12} = \dfrac{(NI)_\mathrm{m}}{R_\mathrm{m} + R_1 + R_2} \dfrac{R_1}{R_{x12}}, \\ \phi_{px21} = \dfrac{(NI)_\mathrm{m}}{R_\mathrm{m} + R_1 + R_2} \dfrac{R_2}{R_{x21}}, \\ \phi_{px22} = \dfrac{(NI)_\mathrm{m}}{R_\mathrm{m} + R_1 + R_2} \dfrac{R_2}{R_{x22}}, \end{cases} \tag{4}$$

where permanent magnet is simply described as magnetomotive force $(NI)_\mathrm{m}$, which depends on its thickness and material properties as in Eq. (5):

$$(NI)_\mathrm{m} = F_\mathrm{c} h_\mathrm{m}, \tag{5}$$

where F_c is the coercive force of the permanent magnet; h_m is magnet thickness; R_m in Eq. (4) is the magnetic resistance of permanent-magnet ring, and it can be written as

$$R_\mathrm{m} = \frac{h_\mathrm{m}}{\mu_0 \mu_\mathrm{r} A_\mathrm{m}}, \tag{6}$$

where the constant μ_r is the relative permeability of permanent magnet, A_m is the cross-section area of the ring permanent magnet.

The R_1 and R_2 in Eq. (4) are given as follows:

$$\begin{cases} R_1 = \dfrac{1}{\dfrac{1}{R_{x11}} + \dfrac{1}{R_{x12}} + \dfrac{1}{R_{y11}} + \dfrac{1}{R_{y12}}}, \\ R_2 = \dfrac{1}{\dfrac{1}{R_{x21}} + \dfrac{1}{R_{x22}} + \dfrac{1}{R_{y21}} + \dfrac{1}{R_{y22}}}, \end{cases} \tag{7}$$

where R_{x11}, R_{x12}, R_{x21}, R_{x22}, R_{y11}, R_{y12}, R_{y21} and R_{y22} are the air gap resistance, and they can be written as follows:

$$\begin{cases} R_{x11}=\dfrac{s_0+x}{\mu_0 A},\ R_{x12}=\dfrac{s_0-x}{\mu_0 A},\ R_{x21}=\dfrac{s_0+x}{\mu_0 A},\ R_{x22}=\dfrac{s_0-x}{\mu_0 A}, \\ R_{y11}=\dfrac{s_0+y}{\mu_0 A},\ R_{y12}=\dfrac{s_0-y}{\mu_0 A},\ R_{y21}=\dfrac{s_0+y}{\mu_0 A},\ R_{y22}=\dfrac{s_0-y}{\mu_0 A}, \end{cases} \tag{8}$$

where the air gap s_0 is the length between the pole surface of rotor and the pole surface of the stator when the rotor is in the centre position; the displacement x is the distance of rotor depart from its centre position on x-axis direction; and the displacement y is the distance of rotor depart from its centre position on y-axis direction.

The control flux of magnetic circuits, ϕ_{cx1}, ϕ_{cx2}, ϕ_{cx21} and ϕ_{cx22}, can be written as follows:

$$\begin{cases} \phi_{cx11}=\phi_{cx21}=\dfrac{Ni_x}{R_{x11}+\dfrac{1}{\dfrac{1}{R_{y11}}+\dfrac{1}{R_{y12}}+\dfrac{1}{R_{x12}}}}+ \\ \qquad \dfrac{Ni_x}{R_{x11}R_{x12}\left(\dfrac{1}{R_{y11}}+\dfrac{1}{R_{y12}}+\dfrac{1}{R_{x11}}\right)+R_{x11}}, \\ \phi_{cx12}=\phi_{cx22}=\dfrac{Ni_x}{R_{x12}+\dfrac{1}{\dfrac{1}{R_{y11}}+\dfrac{1}{R_{y12}}+\dfrac{1}{R_{x11}}}}+ \\ \qquad \dfrac{Ni_x}{R_{x11}R_{x12}\left(\dfrac{1}{R_{y11}}+\dfrac{1}{R_{y12}}+\dfrac{1}{R_{x12}}\right)+R_{x12}}, \end{cases} \tag{9}$$

where N is the number of winding turns, i_x is the control current of poles on x-axis.

Using the Taylor series expansion for small values of x and i_x, we can get the following attractive force with linear terms on x-axis direction:

$$F_x(x, i_x) \cong F_x\big|_{(x_0,\, i_{x0})}+k_i i_x+k_x x. \tag{10}$$

Since the net force is zero at the centre, so Eq. (10) can be rewritten as

$$F_x(x, i_x)=k_i i_x+k_x x, \tag{11}$$

where k_i is the current stiffness and k_x is the negative position stiffness caused by the increasing attractive force as the air gap is reduced. This must be overcome for stable suspension since the homogeneous solution to magnetic bearing force is in the form of hyperbolic functions indicating that x grows with time. k_i and k_x can be calculated as follows:

$$\begin{cases} k_i=\left.\dfrac{\partial F_x}{\partial i_x}\right|_{\substack{i_x=0\\ x=0}}=\dfrac{2F_c h_m N}{\dfrac{h_m s_0}{\mu_0\mu_r A_m}+\dfrac{s_0^2}{\mu_0 A}}. \\ k_x=\left.\dfrac{\partial F_x}{\partial x}\right|_{\substack{i_x=0\\ x=0}}=-\dfrac{\mu_0(F_c h_m)^2}{As_0\left(\dfrac{h_m}{\mu_r A_m}+\dfrac{s_0}{2A}\right)^2}. \end{cases} \tag{12}$$

3.3 Model of the RHMB for tilting

The RHMB also controls two DOFs, viz., tilt about two axes orthogonal to the spin axis when the rotor tilts (besides two DOFs, radial translation along the x and y axes orthogonal to the spin axis). The RHMB creates a tilting stiffness to restrain the rotor when subjected to gyroscopic torque.

When the rotor tilts about an axis orthogonal to the spin axis as shown in Fig. 7, the RHMB will generate required moment to restore its original position. According to the structure of the RHMB and its magnetic circuit (Fig. 4–Fig. 7), the moment produced by middle soft magnetic piece is very small and can be neglected. The moment M acts on the rotor and can be given by Eq. (13).

$$M=L\left(\frac{\phi_{x11}^2}{\mu_0 A}-\frac{\phi_{x12}^2}{\mu_0 A}\right)+L\left(\frac{\phi_{x32}^2}{\mu_0 A}-\frac{\phi_{x31}^2}{\mu_0 A}\right)=2L\left(\frac{\phi_{x11}^2}{\mu_0 A}-\frac{\phi_{x12}^2}{\mu_0 A}\right), \tag{13}$$

where L is the distance from center of the upper or lower magnetic pole to the center of rotor as shown in Fig. 7. The change in air gap is $L\tan\alpha \cong L\alpha$ for small value of the tilting angle α. The air gap resistance can be written as

$$\begin{cases} R_{x11}=\dfrac{s_0+L\alpha}{\mu_0 A},\ R_{x12}=\dfrac{s_0-L\alpha}{\mu_0 A},\ R_{x21}=\dfrac{s_0}{\mu_0 A},\ R_{x22}=\dfrac{s_0}{\mu_0 A}, \\ R_{y11}=\dfrac{s_0}{\mu_0 A},\ R_{y12}=\dfrac{s_0}{\mu_0 A},\ R_{y21}=\dfrac{s_0}{\mu_0 A},\ R_{y22}=\dfrac{s_0}{\mu_0 A}. \end{cases} \tag{14}$$

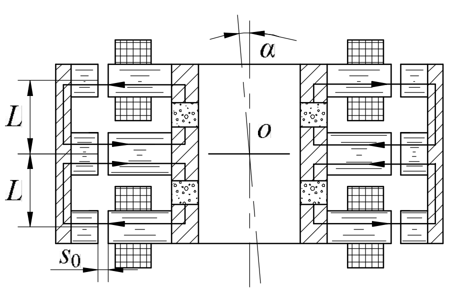

Fig. 7. Tilting movement of the rotor

Using the Taylor series expansion for small values of α and i_x, we can get the following attractive moment with linear terms:

$$M(i_x, \alpha) \cong k_{\alpha i} i_x+k_{\alpha x}\alpha, \tag{15}$$

where $k_{\alpha i}$ is the tilting current stiffness and $k_{\alpha x}$ is the negative tilting position stiffness. They can be calculated as follows:

$$\begin{cases} k_{\alpha i} = \dfrac{\partial M}{\partial i_x} = \dfrac{4}{125} \dfrac{F_c h_m N}{\dfrac{s_0 h_m}{\mu_0 \mu_r A_m} + \dfrac{1}{2} \dfrac{s_0^2}{\mu_0 A}}, \\ k_{\alpha x} = \dfrac{\partial M}{\partial \alpha} = -\dfrac{2}{15\,625} \dfrac{\left(F_c h_m\right)^2}{\mu_0 s_0 A \left(\dfrac{h_m}{\mu_0 \mu_r A_m} + \dfrac{s_0}{2 \mu_0 A_m} \right)^2}. \end{cases} \tag{16}$$

4 Parameters Design and Performance Analysis for the RHMB

4.1 Parameters design for the RHMB

The main parameters of the RHMB are the maximum magnetic force, the current stiffness, and the position stiffness, etc. The performance and application area are decided by these parameters. The RHMB is designed according to the assumed conditions and a 30 N • m • s magnetic bearing wheel (the rotor mass is 6.2 kg) to control the attitude of spacecraft. The main design parameters are shown in Table 1.

Table 1. Design parameters of the RHMB

Parameter	Value
Rotor mass m/kg	6.2
Speed range of wheel rotor n/(r • min^{-1})	±5000
Angular momentum L/(N • m • s)	30 (at 5 kr/min)
Air gap s_0/mm	0.4
Bias flux density in air gap B_{bias}/T	0.445
Number of winding N	200
Area of the magnetic pole face A/mm^2	336
Magnet cross section area A_m/mm^2	424
Magnet thickness h_m/mm	4
Distance from center of the upper/lower magnetic pole to the rotor center S/mm	16

The performance of the RHMB can be calculated according to design parameters (Table 1) and its equivalent magnetic circuits (Fig. 4–Fig. 6). The main performance is shown in Table 2. The current stiffness k_i and the position stiffness k_x are calculated by Eq. (12). The tilting current stiffness $k_{\alpha i}$ and the tilting position stiffness $k_{\alpha x}$ are calculated by Eq. (16).

Table 2. Performance of RHMB

Performance	Value
Current stiffness k_i/(N • A^{-1})	418
Position stiffness k_x/(N • μm^{-1})	−1.032
The maximum force $F_{\max}$/N	206
Tilting current stiffness $k_{\alpha i}$/(N • m • A^{-1})	6.682 7
Tilting position stiffness $k_{\alpha x}$/(N • m • rad^{-1})	−132
The maximum moment M/(N • m)	3.302

4.2 Performance analysis for radial translation of the RHMB

The performance shown in Table 2 is calculated for the rotor center position. The real position of rotor will be controlled within 10 μm. The results are given when the rotor departs −0.02 mm, 0 mm, and 0.02 mm from its centre position, respectively. The relationship between magnetic force and the control current is calculated respectively and is shown in Fig. 8 according to Eq. (3). The magnetic force is nonlinear in proportion to the control current when the rotor departs from its centre position. The magnitude and direction of the rotor departing from its centre position both affect the magnetic force, and the effect is different from the situation when the rotor is in the centre position.

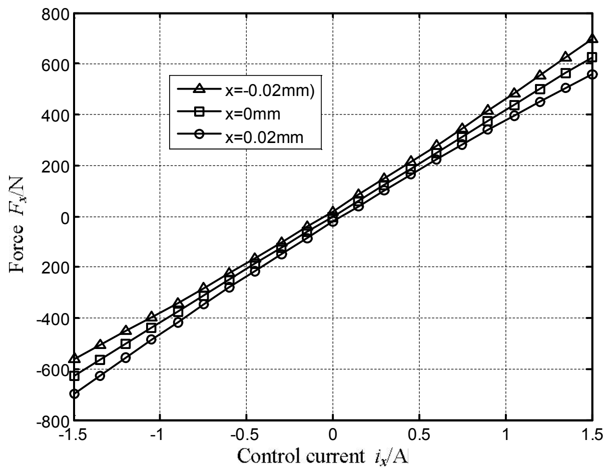

Fig. 8. Bearing force versus control current when the rotor is in different position

The control current will not be 0 A for the real magnetic bearing with disturbing force, and will change according to the movement of the rotor. The results are given when the control current is −0.3 A, 0 A, and 0.3 A, respectively for the RHMB. The relationship between magnetic force and the rotor position is shown in Fig. 9. It is obvious that the magnetic force is nonlinear. The magnitude and direction of the control current both affect its magnetic force. This is a major drawback because much effort of the position controller is necessary to overcome the negative stiffness, limiting the achievable control quality. The position stiffness is −1.032 N/μm.

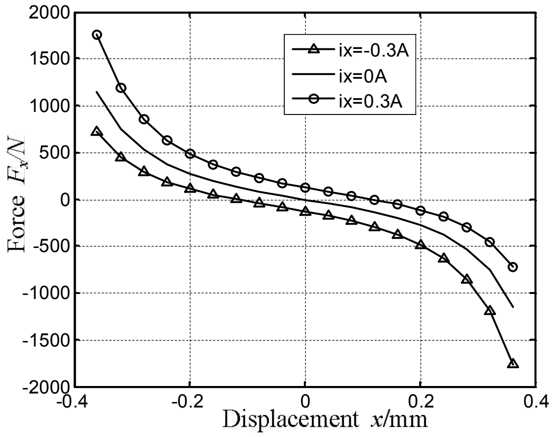

Fig. 9. Bearing force versus displacement with and without control current

In the previous section, the calculated results are given by some given values of control current and the position of rotor. The results shown in Fig. 8 only considered the position of rotor departed −0.02 mm, 0 mm, and 0.02 mm from its centre position. And the results showed in Fig. 9 only considered the control current with −0.3 A, 0 A, and 0.3 A. But the force is affected by the control current and the position of rotor simultaneously.

The following analysis considers all the position of rotor within the clearance space and the control current. The air gap will change from −0.4 mm to 0.4 mm, and the control current will change from −1.5 A to 1.5 A. The curves of the force–current–position characteristic are shown in Fig. 10. It is obvious that the curves of force–current–position characteristic are nonlinear, and the control current and rotor position will affect the magnetic force, current stiffness and position stiffness. But the curve is almost linear for small displacement and control current.

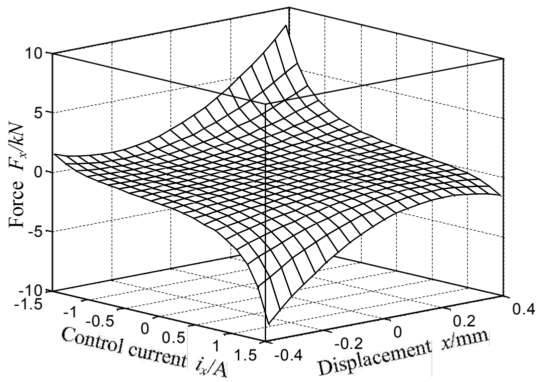

Fig. 10. Characteristic curves of force–current–position for the RHMB

4.3 Performance analysis for tilting of the RHMB

The performance shown in Table 2 is calculated for the rotor center position. The real angular position of rotor will be controlled within 0.02 rad. The results are given when the rotor tilts within −0.02–0.02 rad and −1.5–1.5A, respectively. The relationship among moment, control current, and angular position is calculated by Eq. (13) and Eq. (16). The curves of the moment–current–angular position characteristic are shown in Fig. 11. It is obvious that the curves of moment–current–angular position characteristic are nonlinear, and the control current and rotor angular position will affect the magnetic moment. But the curve is almost linear for small angle and control current.

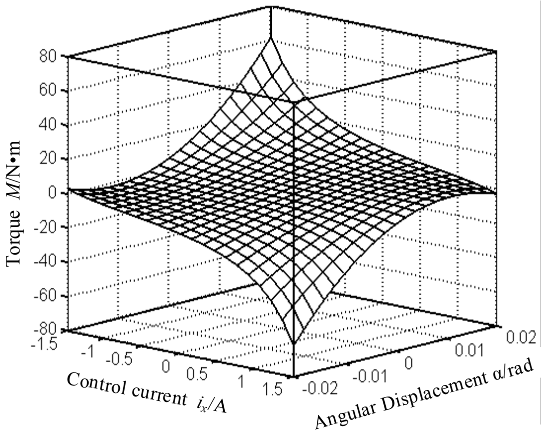

Fig. 11. Characteristic curves of moment–current–angular position for the RHMB

5 Conclusions

(1) A new type of MSRW for high-precise stabilization of spacecraft attitude is introduced and a novel integrated RHMB is designed to reduce the power and minimize the size etc.

(2) The equivalent magnetic circuit model for the RHMB is presented and a solution is found. The stiffness model is also presented, including current stiffness, position negative stiffness, tilting current stiffness, tilting angular position negative stiffness, and force and moment equilibrium equations.

(3) The design parameters of the RHMB are given according to the requirement of the MBRW with angular momentum of 30 N • m • s at 5 kr/min. The nonlinearity of the RHMB is shown by using the characteristic curves of force-current-position, as well as moment-current-angular displacement considering all the rotor position within the clearance space and the control current.

The analysis and design method in this paper can predict all the performance of the radial magnetic bearing with permanent magnet bias, thus can be supplied for design and analysis of magnetic bearings and magnetic bearing wheel system.

References

[1] FEI Congyu, LI Yingtang. Nonlinear control law of satellites attitude at zero-speed of reaction wheels[J]. *Chinese Space Science and Technology*, 2001, 10(5): 21–24. (in Chinese)

[2] HAN Bangcheng, HU Gang, FANG Jiancheng, et al. Optimization design of magnetic bearing reaction wheel rotor[J]. *Journal of Astronautics*, 2006, 27(3): 536–540.

[3] WANG Feng, ZHANG Shijie, CAO Xibin. Research and semi physical simulation for the compensation observer of wheel low speed friction[J]. *Journal of System Simulation*, 2005, 17(3): 613–616. (in Chinese)

[4] FANG Jiancheng, YANG Lei, SUN Jinji, et al. Novel permanent-magnet bias radial magnetic bearing used in magnetical suspended flywheel[J]. *Optics and Precision Engineering*, 2008, 16(3): 444–451. (in Chinese)

[5] YE Q H, LI H, HAN B C, et al. Optimization design of sealed cowling structure for magnetic bearing reaction flyweel[J]. *Optics and Precision Engineering*, 2007, 15(10): 1 571–1 576. (in Chinese)

[6] AUER W. Ball bearing versus magnetic bearing reaction and momentum wheels as momentum actuators[C]//*AIAA International Meeting & Technical Display on Global Technology 2000*, AIAA-80-0911, Baltimore, 1980: 1–5.

[7] FORTESCUE Peter, STARK John. *Spacecraft system engineering*[M]. New York: J. Wiley, 2003.

[8] FAN Yahong, FANG Jiancheng. Experimental research on the nutational stability of magnetically suspended momentum wheel in control moment gyroscope (CMG)[C]//*The Ninth International Symposium on Magnetic Bearings*, USA, 2004: 116–121.

[9] YASUSHI Horiuchi, MASAO Inoue. Development of magnetic bearing momentum wheel for ultra-precision spacecraft attitude control[C]//*The Seventh International Symposium on Magnetic bearings*, ETH Zurich, 2000: 525–503.

[10] ATSUSHI Nakajima. Research and development of magnetic bearing flywheels for attitude control of spacecraft[C]//*Magnetic Bearings Proceedings of the First International Symposium*, Switzerland, 1988: 3–12.

[11] ICHIJU Satoh, JINZO Nagahiro, CHIKARA Nurakami, et al. Vibration and control in outer rotor type magnetic bearings [C]//*Magnetic Bearings Proceedings of the First International Symposium*, Switzerland, 1988: 169–176.

[12] RAJAGOPAl K R, SIVADASAN K K. Low-stiction magnetic bearing for satellite application[J]. *Journal of Applied Physics*, 2002, 91(10): 6 694–6 696.

[13] GAUTHLER M, ROLAND J P, VAILLANT H et al. An advanced low-cost 2-axis active magnetic bearing flywheel [C]//*Proceedings of the 3rd European Space Mechanisms & Tribology Symposium*, Madrid, Spain, 1987: 177–182.

[14] BICHLER U, ECKARDT T. A 3(5) degree of freedom electrodynamic-bearing wheel for 3-axis spacecraft attitude control application[C]//*Magnetic Bearings Proceedings of the First International Symposium*, Switzerland, 1988: 15–22.

Biographical notes

HAN Bangcheng, born in 1974, is currently an associate professor in Beihang University, China. He received his PhD degree from Changchun Institute of Optics, Fine Mechanics and Physics, Chinese Academy of Sciences, China, in 2004. His research interests include mechanotronics engineering, magnetic bearing system, magnetic bearing flywheel and control moment gyroscope.

Tel: +86-10-82317078; E-mail: hanbangcheng@buaa.edu.cn